Ultrasonic Storage Modulus as a Novel Parameter for Analyzing Protein-Protein Interactions in High Protein Concentration Solutions: Correlation with Static and Dynamic Light Scattering Measurements

Atul Saluja,* Advait V. Badkar,† David L. Zeng,† Sandeep Nema,† and Devendra S. Kalonia*
*Department of Pharmaceutical Sciences, School of Pharmacy, University of Connecticut, Storrs, Connecticut 06269; and †Global Biologics, Pfizer Global Research and Development, Chesterfield, Missouri 63017

ABSTRACT The purpose of this work was to establish ultrasonic storage modulus (G') as a novel parameter for characterizing protein-protein interactions (PPI) in high concentration protein solutions. Using an indigenously developed ultrasonic shear rheometer, G' for 20–120 mg/ml solutions of a monoclonal antibody (IgG_2), between pH 3.0 and 9.0 at 4 mM ionic strength, was measured at frequency of 10 MHz. Our understanding of ultrasonic rheology indicated decrease in repulsive and increase in attractive PPI with increasing solution pH. To confirm this behavior, dynamic (DLS) and static (SLS) light scattering measurements were conducted in dilute solutions. Due to technical limitations, light scattering measurements could not be conducted in concentrated solutions. Mutual-diffusion coefficient, measured by DLS, increased with IgG_2 concentration at pH 4.0 and this trend reversed as pH was increased to 9.0. Second virial coefficient, measured by SLS, decreased with increasing pH. These observations were consistent with the nature of PPI understood from G' measurements. Ultrasonic rheology, DLS, and SLS measurements were also conducted under conditions of increased ionic strength. The consistency between rheology and light scattering analysis under various solution conditions established the utility of ultrasonic G' measurements as a novel tool for analyzing PPI in high protein concentration systems.

INTRODUCTION

Protein-protein interactions (PPI) are critical determinants of protein behavior in a solution, be it a pharmaceutical liquid protein formulation or a physiological fluid (1–3). Often, the concentration of proteins in these solutions exceeds the dilute solution regime and they occupy large volume fractions (0.1 and higher) of the solutions (4,5). These solutions are thus classified as concentrated solutions if a single solute is present in high concentration or as crowded solutions if a solute is present in a concentrated solution of another solute. Solution formulation of monoclonal antibodies is a good example of concentrated solutions. Application of monoclonal antibodies for therapeutic purposes, especially in the fields of oncology and immunology, often necessitates preparation of high concentration solutions of these proteins (6,7). In such solution formulations, PPI not only govern the physical properties of the solution like osmotic pressure, diffusion coefficient, viscosity, etc., but also govern its stability against reversible and irreversible processes including association, aggregation, and amorphous precipitation during early production and purification as well as during long-term storage (8). Biological fluids offer examples in which proteins are present in crowded solutions. Muscle cells contain ~23% protein by weight, and red blood cells have ~35% protein by weight (9). Eye lens contains crystallin proteins at concentrations of 20–50% by weight (10). PPI in these biological fluids play a crucial role in the etiology of various diseases and disorders. Examples include cataract, due to aggregation and precipitation of lens crystallins (11), neurodegenerative diseases including Alzheimer's and Parkinson's disease, due to amyloid fibril deposition (12), systemic amyloidosis (13), polyglutamine disorders like Huntington's disease, and diseases of the peripheral tissue like the familial amyloid polyneuropathy (14). Thus, to gain an insight and appreciate the significance of intermolecular interactions in governing such physical and physiological phenomenon, it becomes imperative to characterize the nature of PPI in concentrated conditions. However, currently available techniques for characterization of PPI are limited to dilute solution analysis.

Over the recent past, we have been involved with the analysis of solution rheology of high concentration protein solutions using an indigenously developed shear rheometer capable of working at ultrasonic frequencies (15–17). The broad objective of our work has been targeted toward the generation of a novel tool/parameter for characterizing PPI in high protein concentration solutions. Our studies have indicated that ultrasonic storage modulus (G'), a measure of fraction of applied energy stored by a system, can provide valuable information regarding the nature of PPI in high concentration protein solutions. The reasons for believing that such a correlation between solution G' and PPI could exist can be better appreciated if we briefly review the molecular origins of flow properties of a liquid.

The viscosity, or resistance to flow, of a fluid is a result of momentum transfer between the flowing layers which itself is a result of molecular interactions, i.e., the viscosity of a

Submitted August 11, 2006, and accepted for publication September 19, 2006.

Address reprint requests to Devendra S. Kalonia, Dept. of Pharmaceutical Sciences, School of Pharmacy, University of Connecticut Unit-3092, 69 North Eagleville Road, Storrs, CT 06269. Tel.: 860-486-3655; Fax: 860-486-4998; E-mail: kalonia@uconn.edu.

0006-3495/07/01/234/11 $2.00

doi: 10.1529/biophysj.106.095174

system, is determined by how molecules, which constitute the system, interact. Any movement of molecules (e.g., rotational, translational etc.) or interaction between them is associated with a temperature-dependent relaxation process characterized by a relaxation time (τ). For pure liquids, τ ranges from 10^{-14} to 10^{-11} s (18). Liquid water has a τ of $\sim 10^{-12}$ at 25°C (19). In solutions, additional relaxation processes involving solute-solute and solute-solvent interactions exist that are associated with their characteristic τ. Rotational and translation diffusion of protein molecules in solutions, segmental motions, and conformational rearrangements occur on the timescale of 10^{-7}–10^{-9} s (20–26). Relaxation of bound water occurs around 10^{-10}–10^{-11} s (27). The timescale of these relaxations is governed not only by temperature but also by the solvent and solute concentration. PPI affect conformational rearrangements and segmental motions in protein solutions and thus alter their characteristic τ, e.g., strongly interacting systems (high viscosity solutions of partially unfolded protein and protein gels) exhibit increased values of τ over weakly interacting systems.

Dynamic rheology experiments involving applications of oscillatory strain to the sample can be employed to determine τ. The frequency of the applied strain is utilized to gain insight into the relaxation process in these studies. For studying processes at timescales of 10^{-7}–10^{-9} s, measurements at MHz frequencies need to be conducted, since $1/\omega$ should be of the order of τ of the process. Ultrasonic rheometry is a powerful technique for nondestructive analysis (28) of processes relaxing at nanosecond scales (29,30). The pioneering work in this field was done by Mason and co-workers (31), who studied viscosity and high-frequency elasticity of several polyisobutylene fluids at ultrasonic frequencies by employing quartz crystal vibrating in the torsional and shear modes. Since then, the technique has evolved as a nonconventional means of assessing rheological characteristics of various fluids. In principle, ultrasonic rheometers (32,33) measure the storage (G') and loss (G'') modulus of liquids that characterize elastic storage and viscous loss of energy in a solution, respectively. The moduli are related to the fundamental τ of the liquid through the following relationships (34):

$$G' \propto \frac{\omega^2\tau^2}{1+\omega^2\tau^2} \tag{1}$$

$$G'' \propto \frac{\omega\tau}{1+\omega^2\tau^2}. \tag{2}$$

When $\tau \ll 1/\omega$, i.e., when lower frequency strain is applied, molecules have enough time to reorient and relax within a single strain cycle, resulting in complete dissipation or loss of the applied energy. Consequently, G'' has a finite value but G' is nonexistent. As $1/\omega$ decreases, i.e., ω increases and approaches τ, $\omega\tau \rightarrow 1$, molecules cannot relax completely and the system begins to store a part of the applied energy resulting in a finite value of G'.

Macromolecules in solution are dynamic molecules with numerous randomly contorted conformations that are continuously changing. In dilute solutions, the average conformation of such a molecule is determined by the relative energy minima of various isomeric conformations. The rapidity with which the conformations change is determined by solute-solvent interactions. In concentrated or crowded solutions, interparticle interactions significantly affect the selection of the thermodynamically stable state as well as the rate of change in molecular conformations (35). Thus, a relaxation process in macromolecular solutions usually exhibits a spectrum of relaxation times instead of a single discreet relaxation time (35,36). The moduli for macromolecular solutions are thus represented as

$$G' \propto \sum_{i=1}^{N} \frac{\omega^2\tau_i^2}{1+\omega^2\tau_i^2} \tag{3}$$

$$G'' \propto \sum_{i=1}^{N} \frac{\omega\tau_i}{1+\omega^2\tau_i^2}, \tag{4}$$

with the relative contribution of each relaxation process to solution modulus (or viscosity) dependent on frequency of analysis.

In protein solutions, PPI affecting τ can be studied through the measurement of dynamic moduli at frequencies consistent with the τ of the relaxation processes. Single-frequency measurements can be used to determine change in moduli with solution condition, and thus assess the effect of solution condition on the relaxation process, as long as the frequency is close to the average τ of the relaxation spectrum ($1/\omega$ is an order of magnitude around τ) and not orders of magnitude away from it (35). If the frequency is too low, G' is nonexistent or negligibly small and G'' is insensitive to solution conditions. If the frequency is too high, the moduli approach limiting values, thereby compromising sensitivity to the changing solution environment. In principle, either of the two moduli can give information regarding the changing τ of the system. However, in the frequency domain around τ, such that $0.1 \leq \omega\tau \leq 10$, G'' first increases and then decreases with increasing τ (as $\omega\tau \rightarrow 1$ and then exceeds 1) (Eq. 2) but G' constantly increases with τ (Eq. 1). Thus, whereas an increase in τ of a system will always result in an increasing G', it may result in an increasing or decreasing value of G''. Consequently, G' is a more reliable parameter for predicting and understanding change in PPI in protein solutions from single frequency rheology measurements. From this brief introduction, it can be gathered that for protein solutions, G' measurements at MHz frequencies, consistent with a timescale of 10^{-7}–10^{-9} s, should provide information regarding PPI in these solutions.

Techniques for characterizing PPI in relatively dilute solutions include among others analytical ultracentrifugation, static light scattering (SLS), and dynamic light scattering (DLS). SLS has been routinely used for measurement of a thermodynamic nonideality parameter, i.e., second virial coefficient (B_{22}) which characterizes solute-solute interactions and indirectly solute-solvent interactions (37,38). B_{22}, a

dilute solution property, has been found to correlate remarkably well with protein solubility (39,40), crystallization (37,41) and protein precipitation (42) from supersaturated solutions. It is an established parameter for characterizing PPI in protein solutions. Zimm (43) in 1946 studied the osmotic second virial coefficient of protein to quantitate the deviation from ideality of a dilute solution. The osmotic pressure ($\prod$) of dilute solution follows Eq. 5, which reduces to a van't Hoff relation for an ideal solution when B_{22} vanishes:

$$\Pi = RTc\left(\frac{1}{M_w} + B_{22}c + \ldots\ldots\right). \quad (5)$$

In the above equation, R is the universal gas constant, T is the absolute temperature, c is the solute concentration, and M_w is the average molecular weight. Whereas the value of B_{22} reflects the magnitude of deviation from ideality, its sign reflects the nature of this deviation. A positive value corresponds to net repulsive interactions between the solute molecules wherein the osmotic pressure increases above that for an ideal solution whereas a negative value corresponds to net attractive interactions between the solute molecules with a consequent decrease in solution osmotic pressure below that for an ideal solution (44). In terms of a solute's activity in solution, B_{22} can be related to the molar activity coefficient (γ_2) by the following relationship (45):

$$\gamma_2 = \exp\left(2B_{22}c + \frac{3}{2}B_{222}c^2 + \ldots..\right), \quad (6)$$

where B_{222} represents the third osmotic virial coefficient corresponding to interaction of three solute molecules.

DLS measures the diffusion coefficient of a solute molecule in solution. The diffusion coefficient depends on the hydrodynamic diameter (d_H) of a solute molecule and interparticle repulsive and attractive forces (46,47). For solutions in which interparticle interactions are too weak to influence the diffusion of the solute particle, the diffusion coefficient is independent of solute concentration and the measured d_H is an absolute d_H. However, for strongly interacting solute systems, the so-called mutual-diffusion coefficient (D_m) is concentration-dependent and approaches a self or tracer diffusion coefficient (D_s) under infinitely dilute solution conditions with $c \rightarrow 0$, i.e., in a strongly interacting system, the measured d_H is an apparent diameter that approaches the true particle diameter as $c \rightarrow 0$ (48,49). Therefore, D_s measures the true d_H and D_m measures an apparent d_H of the solute particle. The dependence of D_m on solute concentration can be represented by the following relationship (50):

$$D_m = D_s(1 + k_D c), \quad (7)$$

in which, k_D ($\propto$slope) is a measure of interparticle interaction and is represented by (50,51)

$$k_D = 2B_{22}M_w - \zeta_1 - 2\upsilon_{sp}, \quad (8)$$

where ζ_1 is the coefficient of the linear term in the virial expansion of the frictional coefficient as a function of solute concentration, and υ_{sp} is the partial specific volume of the solute. The contribution of B_{22} to k_D arises from the role of chemical potential in driving the diffusion process, whereas the last two terms represent the hydrodynamic drag (52,53). A positive value of k_D results in an increase in D_m over D_s, which translates to a decrease in the apparent d_H through the Stokes-Einstein equation (Eq. 9), indicating a facilitation of the diffusion of the solute and thus repulsive interparticle interactions:

$$D_m = \frac{kT}{3\pi\eta d_H}. \quad (9)$$

In Eq. 9, k is the Boltzmann constant, T is the absolute temperature, and η is the solution viscosity. A negative value of k_D results in a decrease in D_m below D_s, which translates to an increase in the apparent d_H through the Stokes-Einstein equation, indicating an inhibition of diffusion of the solute and thus attractive interparticle interactions.

The work presented here was undertaken to investigate if the understanding generated from ultrasonic G' measurements regarding PPI in moderate to high concentration solutions of a model protein, a monoclonal antibody (IgG_2) could be corroborated with classical techniques for analyzing PPI, i.e., SLS and DLS in relatively dilute solutions. The reasons for using two different concentration regimes were twofold. First, we wanted to compare our ultrasonic G' results with classical and universally accepted parameters for characterizing PPI, which are B_{22} and k_D. This was necessary to establish the utility of ultrasonic G' for analyzing PPI. However, both these parameters characterize nonideality in dilute rather than concentrated solutions. Second, currently available biophysical techniques for characterization of macromolecular interactions do not permit analysis of concentrated protein solutions due to contribution of higher order coefficients in the virial expansion of solute properties, i.e., osmotic pressure, diffusion coefficient, and frictional coefficient. Quantitation of higher order coefficients is not trivial.

It is well-appreciated in the literature that an accurate quantitation of a concentrated solution property cannot be made based on dilute solution measurements because of the contribution of higher coefficients. However, in most cases the qualitative effect of changing solution conditions on protein behavior can be expected to be similar for dilute and concentrated solutions, with the PPI becoming stronger in concentrated solutions. This is because the fundamental properties of a molecule-like net charge, volume, hydrophobicity, etc., that eventually govern the PPI, do not usually change with concentration. This however, does not undermine the significance of measurements in high concentration solutions since differences in PPI, as a function of changing solution condition, might not be measurable or be insignificant in dilute protein solutions, whereas they might become

significant and large in concentrated solutions. Besides, if the conformation and/or geometry of a molecule were to change with concentration, it would further necessitate analysis of PPI under intended concentrated solution conditions.

MATERIALS AND METHODS

Materials

The monoclonal antibody was generously donated by Pfizer Biologics (St. Louis, MO) and was supplied as a 11.3 mg/ml solution in a 20 mM acetate buffer (pH 5.5) containing 140 mM NaCl and 0.02% w/v polysorbate 20. The monoclonal antibody was an IgG_2, with κ-light chains and a molecular weight of 144,000. Measurements for isoelectric point determination revealed four bands between pH 8.75 and 9.25 on the isoelectric focusing gel. The supplied stock solution was stored at 4°C. All other chemicals including, sodium chloride, acetic acid, sodium acetate, monobasic, and dibasic sodium phosphate and tris(hydroxymethyl) aminomethane, hydrochloric acid, and sodium hydroxide were obtained from Fisher Scientific (Fair Lawn, NJ). Deionized water equivalent to Milli-QTM grade was used to prepare all solutions. Millipore's (Billerica, MA) Amicon Ultra centrifugation tubes with a molecular weight cutoff of 5,000 were obtained from Fisher Scientific.

Methods

For the purpose of this work, analysis was conducted at a temperature of 25° ± 0.1°C. Phosphoric acid-monobasic sodium phosphate (pH 3.0), acetic acid-sodium acetate (pH 4.0, 4.7, 5.4, and 5.9), monobasic-dibasic sodium phosphate (pH 6.4 and 7.4), and tris(hydroxymethyl) aminomethane-hydrochloride (pH 9.0) buffers were prepared to maintain the solution pH. The buffer strength was 10 mM for 40 mM and 300 mM ionic strength buffers and 1 mM for 4 mM ionic strength buffers. The ionic strength was adjusted with sodium chloride. The procedure for sample preparation is described in a recent publication (15).

Ultrasonic shear rheometry

Measurements of G' for the model IgG_2 solutions by ultrasonic rheometry were conducted in a previous work (15). A brief description of the rheometer is included here. An ultrasonic shear rheometer capable of operating at MHz frequencies has been developed in our laboratory (16). The instrument can perform fast analysis of solution rheology of small microliter sample volumes and allows for calculation of solution viscosity, G' and G''. The rheometer is based on a piezoelectric quartz crystal, which is sensitive to the mechanical properties of the liquid placed on top of it. The change in mechanical properties of a liquid including its viscosity and moduli can be determined by measuring the change in the crystal's conductance (G) and the series resonance frequency (f_{Gmax}), defined as the frequency where the conductance of the crystal is the highest, after loading the liquid on the crystal. These two parameters are used to calculate the change in the series resistance (R) and reactance (X) of the crystal brought about by the liquid, i.e., R_{Liq} and X_{Liq}. The following equations can then be used to determine the moduli of the liquid in which A is the electromechanical calibration constant determined separately using water-glycerol mixtures of known density and viscosity and ρ_{Liq} is the density of the liquid:

$$G' = \frac{R_{Liq}^2 - X_{Liq}^2}{A^2 \rho_{Liq}} \tag{10}$$

$$G'' = \frac{2R_{Liq}X_{Liq}}{A^2 \rho_{Liq}}. \tag{11}$$

The measurement setup is enclosed in a circulating water bath for temperature control of the sample droplet. For further details, the interested reader is referred to recent publications (15–17) regarding the development of the instrument and its applications. Ultrasonic rheology studies, for measurement of G' and G'', were conducted at 25 ± 0.1°C on IgG_2 solutions ranging in concentrations from 20 to 120 mg/ml using the developed rheometer.

Dynamic light scattering

DLS studies were conducted on Malvern Instruments' (Worcestershire, UK) Zetasizer Nano S at 25° ± 0.1°C. For DLS analysis, the buffers were filtered through sterile 0.1 μm Millipore's Millex-W syringe filters before dialysis. After dialysis, the concentration of IgG_2 in the solution was adjusted to 12 mg/ml and pH was checked to ensure consistency with the desired pH. The protein solutions were then centrifuged on a Costar (Cambridge, MA) minicentrifuge at 5600 × g for 10 min before analysis. The Malvern Zetasizer Nano S utilizes a 632.8 nm Helium-Neon laser and analyzes scattered light at an angle of 173° by utilizing a novel Non-Invasive Back-Scatter technique. Back-scatter measurement reduces interference from multiple scattering as the light beam does not travel through the entire sample solution and thus allows for higher concentrations solutions to be analyzed. It also limits the interference from dust particles, which behave as large particles and do not scatter significantly in the back direction. Malvern Instruments' DTS2145 low volume glass cuvette was used for holding the sample. The sample volume used for analysis was 70 μl. A total of 10 scans, each with a duration of 5 s, were accumulated for each sample analyzed. Samples were analyzed at 4, 8, and 12 mg/ml for each solution condition. All the samples were analyzed in triplicate. The viscosity of each solution was measured on the ultrasonic shear rheometer and was used in the calculation of D_m. Malvern's DTS software analyzes the acquired correlogram (correlation function versus time) for calculation of hydrodynamic diameter (d_H). The measured d_H can then be used in the Stokes-Einstein equation for calculation of D_m.

Static light scattering

SLS studies were conducted on Precision Detector's (Bellingham, MA) PDDLS Cool Batch system connected to a PD2000DLS light scattering detector through a 5-μm optical cable. For SLS analysis, all the buffers were filtered through Millipore's 0.05-μm membrane filters before dialysis. After dialysis, protein solutions were filtered through Whatman's (Florham Park, NJ) 0.2-μm syringe filters, and IgG_2 concentration was adjusted to 6 mg/ml. The protein solutions were then centrifuged on a Costar minicentrifuge at 5600 × g for 10 min before analysis. The PDDLS Cool Batch uses an 800 nm laser light source and detects scattered light at 90° from 0.03 μl volume of the sample solution. A standard quartz cuvette with a capacity of 850 μl was used as the sample holder. A minimum volume of 100 μl was required for analysis with the cuvette used. Scattered intensity was accumulated at intervals of 1 s for a period of 60 s. Scattered intensity >3% of the average scattered intensity was regarded as noise and not used during further averaging. This was done to reduce the contribution of dust particles to the average scattered intensity. Samples were analyzed at 6 mg/ml and then sequentially diluted to lower concentrations to get at least seven concentration points for each solution condition. All the samples were analyzed in triplicate. The acquired scattered intensities were used to calculate B_{22} by constructing the Debye plot according to the following equation:

$$\frac{Kc}{R_\theta} = \frac{1}{M_w} + 2B_{22}c, \tag{12}$$

where K is the optical constant given by

$$K = \frac{[2\pi n(dn/dc)]^2}{N_A \lambda_0^4}. \tag{13}$$

In the above equations, R_θ is the excess Rayleigh ratio, i.e., a measure of light scattered by the solute; n is the solvent refractive index; dn/dc is the refractive index increment of the solute; N_A is the Avogadro number; and λ_0 is the wavelength of the incident light. For conversion of scattered intensity to Rayleigh ratio, a conversion factor, A, was calculated as follows: A standard IgG molecule of known molecular weight was analyzed on a size exclusion chromatography column connected in series to a dual detector cell assembly, housing an ultraviolet and light scattering detector, and a refractive index detector (54). The setup allows for calculation of dn/dc of a solute in a given solution condition as defined by the mobile phase. The mobile phase used for this purpose was pH 5.4, 40 mM, acetate buffer. Once the dn/dc was calculated (0.184), the optical constant K for the static light scattering instrument was calculated using Eq. 13. Equation 12 can then be written as

$$\frac{Kc}{(I_P - I_B)A} = \frac{1}{M_w} + 2B_{22}c, \tag{14}$$

where I_P is the scattered intensity from the protein solution, I_B is the scattered intensity from solvent, i.e., the buffer and A is the Rayleigh ratio conversion factor. A series of concentration of the standard IgG were then analyzed for scattered intensity (I_P and I_B) on PDDLS Cool Batch in pH 5.4, 40 mM, buffer and constant A was calculated from intercept (as M_w was known). For the model IgG_2, dn/dc values for different solution conditions were determined on the triple detector size-exclusion chromatography set up as detailed above for the standard IgG. For different buffers studied, dn/dc values for the model IgG_2 ranged between 0.183 and 0.187. Thus, an average value of 0.185 was used for calculation of constant K. This value for dn/dc was also found to be consistent with the value reported for IgG in the literature (55,56). The solvent refractive index, n, values for the buffers used were taken from literature (57).

RESULTS AND DISCUSSION

Fig. 1 *a* shows the change in solution G' with IgG_2 concentration at different pH. An existence of G' for most of these solutions indicates that they behave as viscoelastic liquids at the frequency employed for measurement and are unable to lose all the applied energy by flowing with the applied strain. However, solutions at pH 5.4 do not exhibit a measurable solution G' at concentrations below ~60 mg/ml, i.e., these solutions behave as Newtonian liquids at 10 MHz, either because the interactions between the molecules are too weak or the concentration of the interacting molecules is too less for the system to store energy in the allowed time. The same is true for pH 7.4 and 9.0 solutions at and below 40 mg/ml. At concentrations of 40 mg/ml or less, pH 3.0 solutions (and pH 4.0 solutions (15), data shown in Fig. 4 *b*), exhibit a measurable G'. As the concentration of IgG_2 increases, solutions at pH 7.4 and 9.0 begin to exhibit a sharp increase in G' compared to pH 5.4 solutions, with pH 9.0 showing the most dramatic increase. However, pH 3.0 solutions do not exhibit such a steep increase as pH 7.4 and 9.0 although the measured G' stays higher than the corresponding concentration solution at pH 5.4. Solution G' as a function of IgG_2 concentration was also measured at other solution pH between pH 3.0 and 9.0 (data not shown) and pH 5.4 solutions exhibited the minimum G' as compared to corresponding concentration solutions at other pH. Fig. 1 *b* summarizes the effect of pH on solution G' for one such solution concentration, i.e., 120 mg/ml for all the pH studied. This kind of behavior of the model IgG_2 indicates that the nature of interactions governing the storage of energy in IgG_2 solutions is different at solution pH above and below pH 5.4. Solution ultrasonic G' for the model IgG_2 data has been discussed in greater detail in a recent work (15).

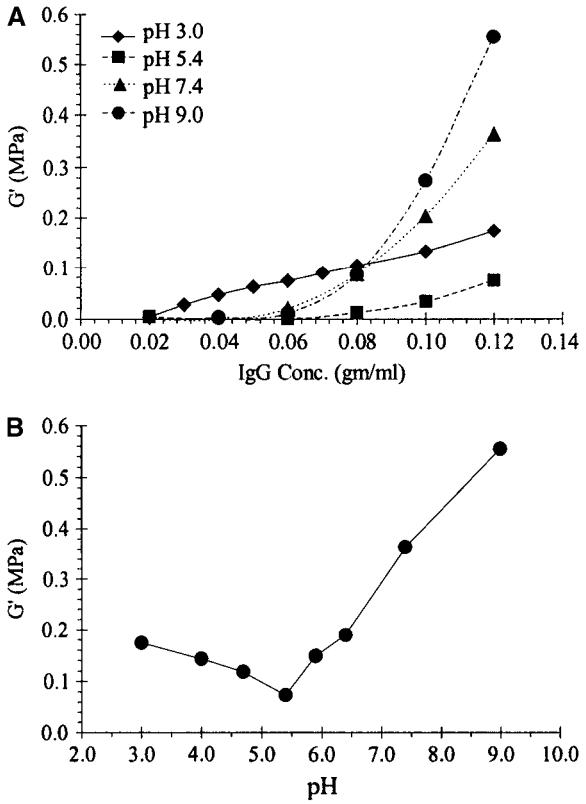

FIGURE 1 Solution storage modulus (G') for IgG_2 solutions at a frequency of 10 MHz measured using the ultrasonic shear rheometer (15) (*a*) as a function of IgG_2 concentration at different solution pH and (*b*) for 120 mg/ml IgG_2 solutions as a function of solution pH. The buffer ionic strength was 4 mM. The line in Fig. 1 *b* connects the points to guide the eye and is not a result of a model fitting to the data. The error bars if not visible are smaller than the symbols used.

In solutions of charged proteins, the sum of the potentials of the mean interparticle forces (W_{22}) contributing to nonideality can be expressed by the following equation (42):

$$W_{22}(r) = W_{hs}(r) + W_{charge}(r) + W_{disp}(r) + W_{osm}(r) + W_{ass}(r) + W_{dip}(r). \tag{15}$$

In the expression, r is the interparticle center-center distance, W_{hs} is the hard sphere (excluded volume) potential, W_{charge} is the electrostatic charge-charge potential, W_{disp} is the van der Waals dispersion potential, W_{osm} is the attractive potential due to the osmotic effect of added salt, W_{ass} is the square-well interaction that accounts for self-association of proteins, and W_{dip} is the interaction due to permanent and induced dipoles. Under low to moderate ionic strength conditions (<0.1 M), W_{osm} is not significant, and other terms in Eq. 15 contribute to the total interparticle interactions. Among these interactions, charge-charge forces, which are

repulsive in nature, play the predominant role in dilute solutions unless the molecules have a tendency to self-associate, when the last term also contributes significantly (42,58) . In concentrated solutions, repulsive-excluded volume effect and attractive van der Waals and dipole forces, all of which are short-range, begin to contribute significantly in addition to charge-charge repulsive forces.

Previous investigation (15) into the contributing interactions responsible for the aforementioned behavior of the model IgG_2 has revealed the contribution of higher effective volume (intrinsic viscosity) and electrostatics (ζ-potential) at lower pH studied in this work. Both intrinsic viscosity and ζ-potential gradually decreased as the pH was increased from 4.0 to 9.0, indicating a decrease in repulsive PPI. In the cited work, pH 9.0 solutions exhibited the greatest scattered light intensity measured at 600 nm and at an IgG_2 concentration of 10 mg/ml, whereas pH 4.0 solutions exhibited the least scattered intensity. Concentrated solutions (120 mg/ml) at pH 9.0 also exhibited slight opalescence, which could not be removed by centrifugation. However, solutions became clear on reducing the solution pH, indicating the presence of some soluble and reversible higher molecular weight species in pH 9.0 solutions at 120 mg/ml. The reversibility of the opalescence also indicated that it was not a result of precipitation or irreversible aggregate formation. Our results thus indicated the gradual transition from highly repulsive PPI to less repulsive or more attractive PPI with increasing pH. To investigate if such an understanding regarding PPI generated from ultrasonic rheology and biophysical characterization studies of IgG_2 solutions was indeed correct, light scattering studies were undertaken.

Fig. 2 *a* shows the effect of solution pH and protein concentration on the measured d_H (apparent) of the model IgG_2 solutions at an ionic strength of 4 mM. Hydrodynamic diameter changes both with solution pH and protein concentration. A decrease in d_H with IgG_2 concentration is observed for pH 4.0 solutions and an increase is observed for pH 9.0 solutions. Using Stokes-Einstein equation, the measured d_H and solution viscosity values were used to calculate D_m for the model IgG_2 molecule. These calculated values have been plotted in Fig. 2 *b* in which the lines represent a linear fit (Eq. 7) to the data. With an increasing solution pH, a decrease in the slope of the plots is observed. In our studies, the average value of the intercept of Fig. 2 *b*, which corresponds to D_s for the model IgG_2, was calculated to be $4.20 \pm 0.16 \times 10^{-7}$ cm^2/s, which corresponds to a d_H of 11.3 ± 0.8 nm. This size is equal (within experimental error) to the d_H reported in the literature for a protein with M_w of ~144,000 (59,60). From Fig. 2 *b*, it can be seen that with increasing solution pH, PPI become more attractive and less repulsive, consistent with the behavior understood from solution G' measurements. During DLS studies, the polydispersity index for all the samples analyzed was ≤ 0.1, which is consistent with a monodisperse sample, i.e., no aggregates were present in the solutions analyzed.

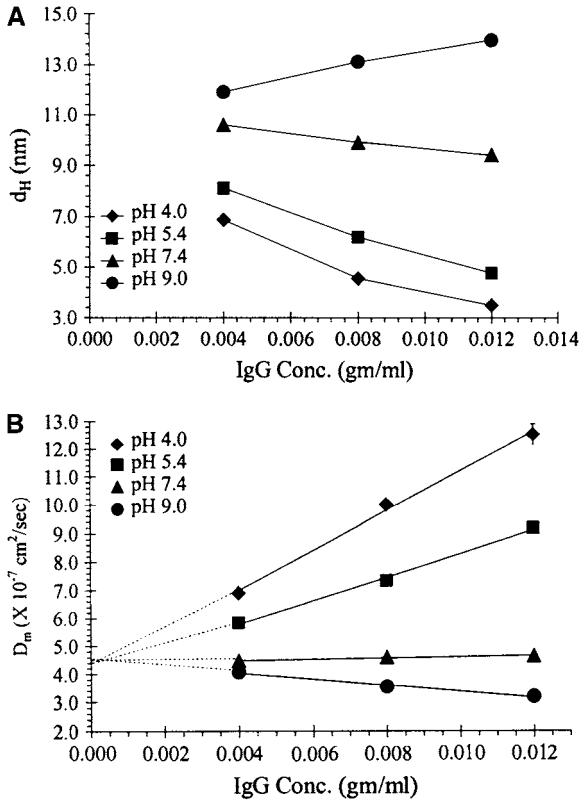

FIGURE 2 (*a*) Hydrodynamic diameter (d_H) and (*b*) mutual-diffusion coefficient (D_m) for IgG_2 molecules as a function of concentration and solution pH at 4 mM ionic strength and 25 ± 0.1°C measured using DLS. The measurements were conducted in triplicate. D_m was back calculated from the measured d_H using the Stokes-Einstein equation (Eq. 9) and solution viscosities measured on the ultrasonic shear rheometer. In Fig. 2 *a*, lines connect the data points and are not a result of model fitting, and in Fig. 2 *b*, lines are linear best fits with the slope and intercept representing $D_s k_D$ and D_s (self-diffusion coefficient), respectively (Eq. 7).

Subsequently, SLS studies were conducted to determine B_{22}, a classical measure of interparticle interactions. Fig. 3 shows the Debye plots for the model IgG_2 solutions at an ionic strength of 4 mM at different solution pH. pH 4.0 solutions exhibit the most positive slope and pH 9.0 solutions exhibit the least positive slope. Unlike DLS measurements (Fig. 2 *b*), the slope of the Debye plot at pH 9.0 is not negative, indicating the net PPI to be less repulsive than pH 4.0 but not attractive. This observation can be explained based on the nature of interactions contributing to SLS and DLS for a macromolecular solution under given experimental conditions. The last two terms in Eq. 8 represent the hydrodynamic interactions (k_H)of the solute molecules, whereas the first term involving B_{22} represents thermodynamic contribution (k_T) involving direct interactions (61,62), i.e.,

$$k_D = k_T - k_H, \tag{16}$$

where

$$k_T = 2B_{22}M_w \tag{17}$$

and

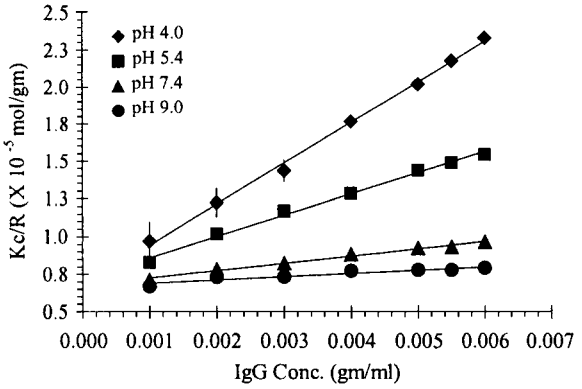

FIGURE 3 Debye plots for IgG_2 solutions as a function of solution pH at 4 mM ionic strength. The second virial coefficient and molecular weight calculated from the slope and intercept, respectively, of the Debye plots have been summarized in Table 1. The measurements were conducted at 25 ± 0.1°C in triplicate for each solution.

$$k_H = \zeta_1 + 2\upsilon_{sp}. \tag{18}$$

Hydrodynamic interactions contribute to calculated diffusivity of molecules in solution in the ''hydrodynamic regime'' (63), which exists when i), the measurement time in DLS (τ_D) is larger than the average collision time (τ_c) between the solute molecules, and ii), the scattering wave number q as represented by Eq. 19 is small enough such that q^{-1} is larger than the center-to-center interparticle distance (64):

$$q = \frac{4\pi n}{\lambda}\sin\left(\frac{\theta}{2}\right). \tag{19}$$

In Eq. 19, n represents the solution refractive index, θ is the scattering angle, and λ is the wavelength of incident light. In our experiments, τ_c for IgG_2 molecules at the lowest concentration used for DLS measurements, i.e., 4 mg/ml, was measured to be $\sim 9 \times 10^{-6}$ s, using Eq. 20 (65), and decreased to $\sim 3 \times 10^{-6}$ s at 12 mg/ml:

$$\tau_c = (4\pi D_s d_H \rho_n)^{-1}. \tag{20}$$

In Eq. 20, ρ_n is the protein number density defined as number of protein molecules per unit volume and is dependent on protein concentration. The τ_D calculated from the decay of the correlation function was $\sim 4 \times 10^{-5}$ s. The center-center distance at 4 mg/ml was calculated as $\rho_n^{-1/3}$ to be ~31 nm, which reduced to ~22 nm at 12 mg/ml, whereas q^{-1} was ~39 nm for our experiments. Therefore, although SLS measurements were affected by thermodynamic interactions, DLS measurements were affected by hydrodynamic interactions in addition to thermodynamic interactions (65). The negative slope at pH 9.0 in Fig. 2 *b* is thus a result of a k_D exceeding k_T. Table 1 summarizes the results for DLS and SLS analysis conducted on the model IgG_2. Although the slopes in Figs. 2 *b* and 3 for pH 9.0 solutions have different signs for the reason explained above, the overall behavior of the IgG_2 in solutions as elucidated by SLS measurements is consistent with DLS measurements, i.e., the PPI are most repulsive at pH 4.0 and least repulsive at pH 9.0. Both k_D and k_T ($\propto B_{22}$) exhibit a monotonic decrease with increasing solution pH.

After conducting these light scattering studies, the behavior of the model IgG_2 in solution can be summarized as follows: Three different kinds of interactions play a role in governing solution behavior of IgG_2 molecules. Long-range charge-charge interactions, which are repulsive in nature, dominate at acidic pH in lower concentration IgG_2 solutions (pH 3.0 and 4.0 solutions exhibit larger G' at lower concentrations). At acidic pH and higher IgG_2 concentrations, both excluded volume and charge-charge interactions predominantly contribute to solution behavior. Specific attractive PPI, the nature of which is yet undetermined, contribute more significantly at pH 7.4 and 9.0 and cause a sharper increase in solution G' as compared to repulsive interactions with increasing IgG_2 concentration. The dominant role of repulsive and attractive interactions switches around pH 5.4 and consequently these solutions exhibit a minimum in solution G'.

To investigate the correlation between G' and PPI further, ultrasonic rheology and light scattering measurements were conducted on IgG_2 solutions of increasing ionic strength at various solution pH. The ionic strength was adjusted with sodium chloride. Fig. 4, *a* and *b*, show the effect of ionic strength on IgG_2 solution G' at different pH. Fig. 4 *a* shows data for 120 mg/ml and Fig. 4 *b* for 40 mg/ml IgG_2 solutions. From Fig. 4 *a*, it can be observed that solution G' increases at pH 4.0 and 5.4, and decreases at pH 9.0 with increasing solution ionic strength. At pH 7.4, such a monotonic increase or decrease in solution G' with ionic strength is not observed as G' decreases from 4 mM to 40 mM and then increases from 40 mM to 300 mM, although G' at 300 mM is still lower than that at 4 mM. It has been discussed earlier in this section that when PPI are highly repulsive (below pH 5.4 from Fig. 1 *a*), G' is higher for solutions with lower concentration of IgG_2. As the interactions become less repulsive and more attractive (with pH increasing above 5.4), solutions with higher IgG_2 concentrations exhibit higher solution G'. From Fig. 4 *b*, it can be observed that at 40 mg/ml, ionic strength does not significantly affect the solution G', although the measured G' is highest at pH 4.0 as mentioned earlier during discussion of Fig. 1 *a*. Therefore, the increase in G' with ionic strength observed for pH 4.0 and 5.4 (Fig. 4 *a*) is a result of PPI becoming less repulsive or more attractive. The increase cannot be due to PPI becoming more repulsive since no significant change was observed for lower IgG_2 concentration solutions (40 mg/ml). For pH 7.4 and 9.0 solutions in Fig. 4 *a*, the predominant effect of ionic strength is to decrease G' at higher protein concentrations, whereas lower protein concentration (Fig. 4 *b*) solutions do not exhibit a significant change in G' with ionic strength. This kind of behavior indicates that the interactions become less attractive or more repulsive with increasing ionic strength with pH 9.0 solutions being affected more than pH 7.4 solutions. However, the

TABLE 1 Parameters calculated for IgG_2 in solution using static and dynamic light scattering measurements at 25 ± 0.1°C. The buffers were formulated at 4 mM ionic strength; each solution was analyzed in triplicate

pH	$D_s \times 10^{-7}$ (cm^2/s)*	d_H (nm)†	$B_{22} \times 10^{-4}$ (mol ml/gm^2)	M_w (×1000)‡	k_D (ml/gm)§	k_T (ml/gm)¶	k_H (ml/gm)‖
4.0	4.19 ± 0.11	11.6 ± 0.3	13.6 ± 1.1	153 ± 17	16.7 ± 0.7	392.4 ± 31	375.7
5.4	4.10 ± 0.03	11.8 ± 0.1	7.1 ± 0.1	139 ± 2	10.1 ± 0.2	202.3 ± 3	192.2
7.4	4.40 ± 0.02	11.0 ± 0.0	2.4 ± 0.1	147 ± 2	0.5 ± 0.1	69.5 ± 2	69.0
9.0	4.47 ± 0.02	10.8 ± 0.0	1.1 ± 0.1	149 ± 3	−2.5 ± 0.1	31.2 ± 1	33.7

*From intercept of plots in Fig. 2 *b*.
†True hydrodynamic diameter calculated at c → 0.
‡From Debye plots (Fig. 3).
§Slope (plots in Fig. 2 *b*)/D_s.
¶Calculated using M_w of 144,000.
‖± SD not given as value calculated is the difference between average k_D and k_T.

increase in repulsive interactions is not large enough to increase G' at lower protein concentrations. Thus, the overall effect of increasing ionic strength is to neutralize the effect of solution pH on PPI and solution rheology in the model IgG_2 solutions (increasing G' at pH 4.0 and 5.4 and making PPI less repulsive or more attractive and decreasing G' at pH 7.4 and 9.0 and making PPI more repulsive or less attractive).

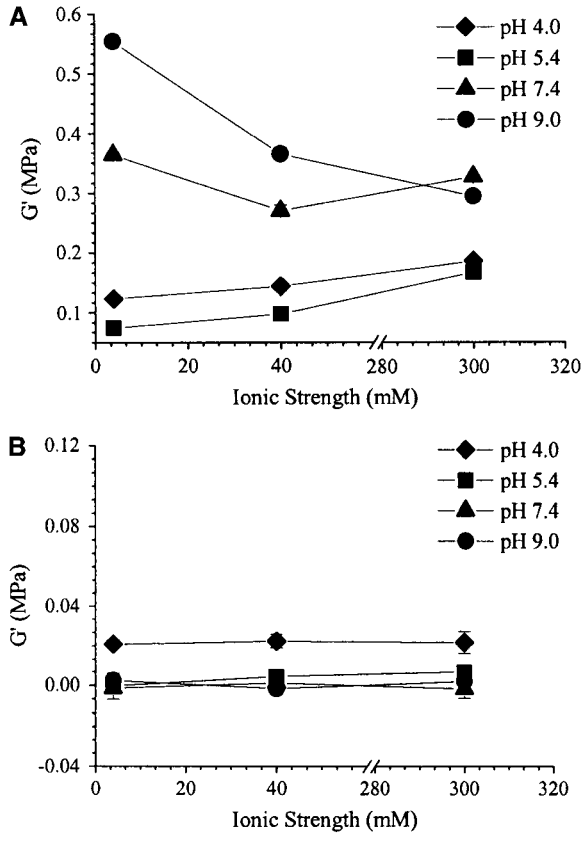

FIGURE 4 Solution G' for IgG_2 solutions at a frequency of 10 MHz measured using the ultrasonic shear rheometer as a function of ionic strength and pH at (*a*) 120 mg/ml and (*b*) 40 mg/ml protein concentration. The ionic strength was adjusted using sodium chloride, and analysis was conducted at 25 ± 0.1°C in triplicate. The error bars if not visible are smaller than the symbols used. A scale break has been included in the *x* axis. The lines connect the points to guide the eye and are not a result of model fitting to the data.

Fig. 5 summarizes the effect of ionic strength on k_D for the model IgG_2 in solutions of different solution pH. A scale break has been included in the *x* axis to compare the low and high ionic strength regions. A more extensive study of the effect of ionic strength on k_D was conducted between 4 mM and 40 mM, with small increments in ionic strength. The reason for this is explained in the next few lines. At pH 4.0 and 5.4, k_D exhibits a steep decrease with increasing ionic strength consistent with decreasing repulsive PPI. At pH 9.0, an increase in k_D is observed with ionic strength, although it stays negative. The behavior at pH 9.0 is consistent with decreasing attractive PPI. However, even at the highest ionic strength studied, k_D does not increase as much or the interactions do not become as repulsive as those exhibited by pH 4.0 and 5.4 solutions at ionic strengths below ~20 mM. Another observation from Fig. 5 is the fact that the effect of pH on solution behavior of IgG_2 is more or less neutralized by 40 mM salt, i.e., the value of k_D → constant value (−1.0 ml/gm in this case) for all the pH studied. Thus, to study the true effect of ionic strength, more salt concentrations were studied in this narrow range from 4 m to 40 mM. Between the ionic strength of 60 mM–300 mM, k_D can be observed to be almost constant.

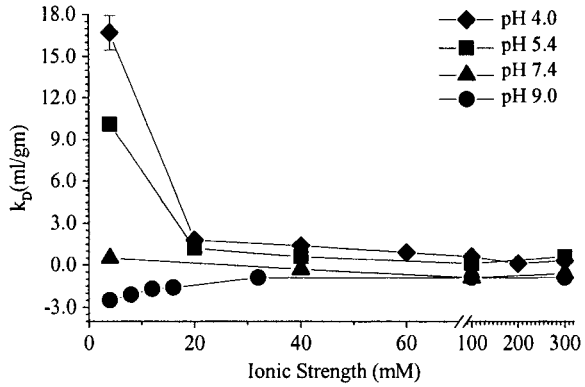

FIGURE 5 Calculated k_D values for IgG_2 molecules in solution of different pH with ionic strength ranging from 4 mM to 300 mM. The ionic strength was adjusted using sodium chloride. The data points have been connected to guide the eye. A scale break has been included in the *x* axis. The lines do not represent the result of model fitting to the data.

Fig. 6 shows the effect of increasing ionic strength on B_{22} of IgG_2 in solution. A scale break has been included in the x axis. Solutions at pH 4.0 and 5.4 show a decrease in B_{22} value with increasing ionic strength, the effect being greater at pH 4.0. These measurements further confirm that increase in ionic strength of these solutions results in a decrease in repulsive PPI. Solutions at pH 9.0 and 300 mM ionic strength show a relatively small increase in B_{22} as compared to lower ionic strength solutions. Although a negative B_{22} was not observed unlike a negative k_D (Table 1) for 4 mM ionic strength solutions at pH 9.0, the effect of ionic strength on B_{22} is consistent with the change in k_D, i.e., increasing repulsive PPI or a decreasing attractive PPI. Consistent with the observations from Figs. 4 and 5, the increase in repulsive interactions at 300 mM is not large enough to result in as positive a B_{22} as those observed for pH 4.0 and pH 5.4 at 4 mM ionic strength. In agreement with the DLS data, an ionic strength of 40 mM is just enough to neutralize any pH-mediated effect on B_{22} of IgG_2 in solution. Thus, there is a strong correlation between the predicted behavior of IgG_2, from G' measurements done on concentrated solutions, and that understood based on DLS and SLS measurements conducted on dilute solutions.

Significance of high concentration measurements

Despite the qualitative correlations observed and discussed above between high concentration G' measurements and dilute solution B_{22} and k_D data, certain differences in the dilute and concentrated solution behavior were also observed for the model IgG_2 solutions. In our studies, opalescence was observed for high concentration solutions of IgG_2 at pH 9.0 and 4 mM ionic strength. The observed opalescence was reversible upon dilution and with changing solution condition. This kind of behavior indicates the presence of attractive PPI in concentrated IgG_2 solutions. The steep increase in solution G' with IgG_2 concentration above pH 5.4 also indicates the presence of strong attractive interactions in concentrated solutions. However, a negative B_{22}, which is believed to be consistent with net attractive PPI, was not observed from dilute solution studies. Such a behavior of the model IgG_2 is similar to the results of a recent work conducted on an IgG_1 molecule (8), which demonstrates the presence of reversible self-association and thus net attractive interactions in high concentration solutions of a monoclonal antibody. In the cited work as well, the B_{22} values measured by the authors were found to be positive (2.3 ± 0.12 ml-mol/gm^2). Although we did not analyze the presence or absence of self-association in concentrated solutions of the model IgG_2, a reversible phenomenon was indeed observed. Due consideration also needs to be given to the interparticle distance (inverse cube root of protein number density, $\rho_n^{-1/3}$) as a function of concentration. The center-center interparticle distance decreases with increasing concentration. For IgG molecules, this distance is ~22 nm at 20 mg/ml and reduces to 12 nm at 120 mg/ml, which is close to the average hydrodynamic size of the molecule. This would signify that at the highest concentration used in our work, surfaces of the molecules are in close proximity to each other, which would enhances the probability of molecular collisions and formation of higher order species of a monomer. The small separation distance also enhances the magnitude of attractive forces including van der Waals and dipole interactions, which are short-range forces as compared to long-range charge-charge repulsive forces.

Fig. 7 demonstrates the difference in dilute and concentrated solution behavior. The figure shows the change in IgG_2 solution G', measured at 120 mg/ml, and k_D values measured from relatively dilute solution analysis, for pH 9.0 solutions as a function of solution ionic strength. Both the parameters exhibit the maximum change with ionic strength up to 40 mM. However, between 40 and 300 mM, whereas solution k_D changes insignificantly (signifying that attractive PPI existing at lower ionic strengths have already been neutralized by

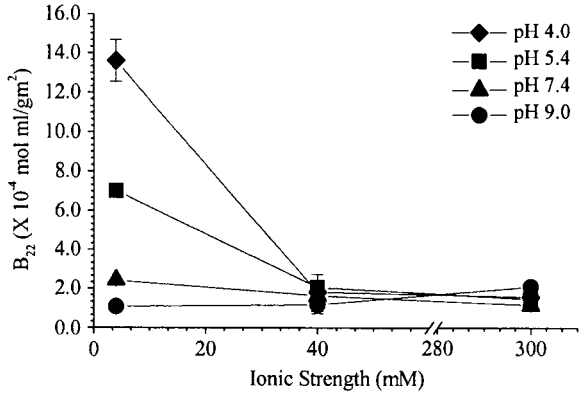

FIGURE 6 B_{22} values for IgG_2 molecules in solutions of different pH as a function of ionic strength. The results are an average of three measurements conducted at 25 ± 0.1°C. A scale break has been included in the x axis. The lines do not represent the result of a model fit to the data.

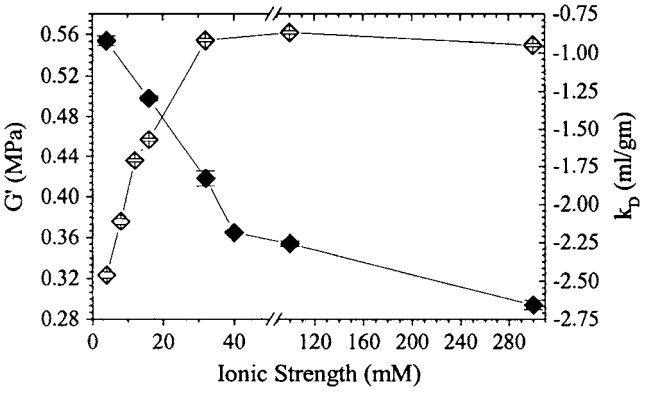

FIGURE 7 Solution G' (♦), at 120 mg/ml IgG_2, and k_D values (◇), calculated from relatively dilute solution measurements (4–12 mg/ml IgG_2), for IgG_2 solutions as a function of solution ionic strength. A scale break has been added in the x axis to focus on low and high ionic strength regions. The lines connect the points to guide the eye and are not a result of a model fit to the data.

40 mM ionic strength), solution G' continues to decrease (a scale break has been incorporated in the x axis in Fig. 7 to focus on low and high ionic strength regions). Similar correlation was observed for other solution pH as well (data not shown) wherein an increase in k_D coincided with a decrease in G' and vice versa up to 40 mM ionic strength after which effect of ionic strength on k_D saturates but G' continues to change with ionic strength. This phenomenon can also be observed from Fig. 6, where the effect of ionic strength, beyond 40 mM, on B_{22} (dilute solution) is much smaller than on solution G' (Fig. 4 *a*, concentrated solution).

The aforementioned observations signify that a measurable effect of a solution variable (pH, ionic strength, excipients, etc.) on a solution property at relatively lower solute concentrations can be used to predict the solution behavior at higher solute concentrations. However, the absence of any such measurable change at lower solute concentrations cannot be a reliable predictor of the solution behavior, with respect to that solution variable at higher solute concentrations. Thus, to understand the behavior of proteins in high concentration and crowded solutions, it is critical to analyze the nature of PPI under the actual concentrated solution conditions. Ultrasonic solution G' measurement can be powerful tool for performing such an analysis.

SUMMARY AND CONCLUSIONS

The storage modulus or G' of a protein solution measured at ultrasonic frequencies can provide valuable information regarding the nature of PPI in concentrated protein solutions. The need for conducting measurements at ultrasonic frequencies arises due to the timescale of movements that occur in protein solutions. These movements are affected by the nature of PPI. These include rotational and translation diffusion of protein molecules in solutions, segmental motions, and conformational rearrangements. The results presented in this work demonstrate the correlation between the nature of PPI as understood and predicted by ultrasonic G' measurements with traditionally used parameters for characterizing PPI, i.e., B_{22} and k_D. An understanding of the behavior of a model protein, a monoclonal antibody (IgG_2), generated from G' measurements agrees well with the light scattering measurements (static and dynamic) of B_{22} and k_D. Since methods for characterization of PPI are limited to the analysis of solutions relatively dilute than those employed for measurement of solution G', the consistency between ultrasonic rheology and light scattering measurements has been established in qualitative rather than quantitative terms. Results presented here also demonstrate that in certain cases where dilute solution analysis fails to capture the effect of solution environment on protein behavior, analysis under higher concentrations can be successfully used to distinguish this effect. Ultrasonic G' measurement is a tool that is applicable to the analysis of PPI in high protein concentration solutions.

The authors thank Dr. James L. Cole for providing access to dynamic light scattering facility and Pfizer for donating the model protein for this study and for partial financial support for this work. The contributions of the Gerald J. Jackson Memorial Foundation at the University of Connecticut and Boehringer Ingelheim Pharmaceuticals in the form of student fellowships are also greatly acknowledged.

REFERENCES

1. Curtis, R. A., J. Ulrich, A. Montaser, J. M. Prausnitz, and H. W. Blanch. 2002. Protein-protein interactions in concentrated electrolyte solutions: Hofmeister series effects. *Biotechnol. Bioeng.* 79:367–380.
2. Minton, A. P. 1983. The effect of volume occupancy upon the thermodynamic activity of proteins: some biochemical consequences. *Mol. Cell. Biochem.* 55:119–140.
3. Lonetti, B., E. Fratini, S. H. Chen, and P. Baglioni. 2004. Viscoelastic and small angle neutron scattering studies of concentrated protein solutions. *Phys. Chem. Chem. Phys.* 6:1388–1395.
4. Hall, D., and A. P. Minton. 2003. Macromolecular crowding: qualitative and semiquantitative successes, quantitative challenges. *Biochim. Biophys. Acta.* 1649:127–139.
5. Rivas, G., and A. P. Minton. 2004. Non-ideal tracer sedimentation equilibrium: a powerful tool for the characterization of macromolecular interactions in crowded solutions. *J. Mol. Recognit.* 17:362–367.
6. Brekke, O. H., and I. Sandlie. 2003. Therapeutic antibodies for human diseases at the dawn of the twenty-first century. *Nat. Rev. Drug Discov.* 2:52–62.
7. Harris, R. J., S. J. Shire, and C. Winter. 2004. Commercial manufacturing scale formulation and analytical characterization of therapeutic recombinant antibodies. *Drug Dev. Res.* 61:137–154.
8. Liu, J., M. D. H. Nguyen, J. D. Andya, and S. J. Shire. 2005. Reversible self-association increases the viscosity of a concentrated monoclonal antibody in aqueous solution. *J. Pharm. Sci.* 94:1928–1940.
9. Fulton, A. B. 1982. How crowded is the cytoplasm? *Cell.* 30:345–347.
10. Pigaga, V., and R. A. Quinlan. 2006. Lenticular chaperones suppress the aggregation of the cataract-causing mutant T5P γC-crystallin. *Exp. Cell Res.* 312:51–62.
11. Stradner, A., G. Thurston, V. Lobaskin, and P. Schurtenberger. 2004. Structure and interactions of lens proteins in dilute and concentrated solutions. *Prog. Colloid Polym. Sci.* 126:173–177.
12. Meehan, S., Y. Berry, B. Luisi, C. M. Dobson, J. A. Carver, and C. E. MacPhee. 2004. Amyloid fibril formation by lens crystallin proteins and its implications for cataract formation. *J. Biol. Chem.* 279:3413–3419.
13. Harper, J. D., and P. T. Lansbury. 1997. Models of amyloid seeding in Alzheimer's disease and scrapie: mechanistic truths and physiological consequences of the time-dependent solubility of amyloid proteins. *Annu. Rev. Biochem.* 66:385–407.
14. Koo, E. H., P. T. Lansbury, and J. W. Kelly. 1999. Amyloid diseases: abnormal protein aggregation in neurodegeneration. *Proc. Natl. Acad. Sci. USA.* 96:9989–9990.
15. Saluja, A., A. V. Badkar, D. L. Zeng, S. Nema, and D. S. Kalonia. 2006. Application of high-frequency rheology measurements for analyzing protein-protein Interactions in high protein concentration solutions using a model monoclonal antibody (IgG_2). *J. Pharm. Sci.* 95:1967–1983.
16. Saluja, A., and D. S. Kalonia. 2004. Measurement of fluid viscosity at microliter volumes using quartz impedance analysis. *AAPS PharmSciTech.* 5:Article 47.
17. Saluja, A., and D. S. Kalonia. 2005. The application of ultrasonic shear rheometer to characterize rheological properties of high protein concentration solutions at microliter volume. *J. Pharm. Sci.* 94:1161–1168.
18. Ronne, C., L. Thrane, P.-O. Astrand, A. Wallqvist, K. V. Mikkelsen, and S. R. Keiding. 1997. Investigation of the temperature dependence of dielectric relaxation in liquid water by THz reflection spectroscopy and molecular dynamics simulation. *J. Chem. Phys.* 107:5319–5331.
19. Endo, H. 1979. Structural relaxation time of liquid water in the two-state model. *J. Chem. Phys.* 71:2464–2466.
20. Camacho, C. J., S. R. Kimura, C. DeLisi, and S. Vajda. 2000. Kinetics of desolvation-mediated protein-protein binding. *Biophys. J.* 78:1094–1105.

21. Buckin, V., and E. Kudryashov. 2001. Ultrasonic shear wave rheology of weak particle gels. *Adv. Colloid Interface Sci.* 89–90:401–422.

22. Pal, S. K., J. Peon, B. Bagchi, and A. H. Zewail. 2002. Biological water. Femtosecond dynamics of macromolecular hydration. *J. Phys. Chem. B.* 106:12376–12395.

23. Hink, M. A., T. Bisseling, and A. J. W. G. Visser. 2002. Imaging protein-protein interactions in living cells. *Plant Mol. Biol.* 50:871–883.

24. Howard, M. J., H. J. Chauhan, G. J. Domingo, C. Fuller, and R. N. Perham. 2000. Protein-protein interaction revealed by NMR T_2 relaxation experiments: the lipoyl domain and E1 component of the pyruvate dehydrogenase multienzyme complex of bacillus stearothermophilus. *J. Mol. Biol.* 295:1023–1037.

25. Phizicky, E. M., and S. Fields. 1995. Protein-protein interactions: methods for detection and analysis. *Microbiol. Rev.* 59:94–123.

26. Rajamani, D., S. Thiel, S. Vajda, and C. J. Camacho. 2004. Anchor residues in protein-protein interactions. *Proc. Natl. Acad. Sci. USA.* 101:11287–11292.

27. Hayashi, Y., N. Miura, N. Shinyashiki, S. Yagihara, and S. Mashimo. 2000. Globule-coil transition of denatured globular protein investigated by a microwave dielectric technique. *Biopolymers.* 54:388–397.

28. Rouse, P. E., Jr. 1998. A theory of the linear viscoelastic properties of dilute solutions of coiling polymers. II. A first-order mechanical thermodynamic property. *J. Chem. Phys.* 108:4628–4633.

29. Nwankwo, E., and C. J. Durning. 1998. Impedance analysis of thickness-shear mode quartz crystal resonators in contact with linear viscoelastic media. *Rev. Sci. Instrum.* 69:2375–2384.

30. Reddy, S. M., J. P. Jones, and T. John Lewis. 1997. Use of combined shear and pressure acoustic waves to study interfacial and bulk viscoelastic effects in aqueous polymeric gels and the influence of electrode potentials. *Faraday Discuss.* 107:177–196.

31. Mason, W. P., W. O. Baker, H. J. McSkimin, and J. H. Heiss. 1949. Measurement of shear elasticity and viscosity of liquids at ultrasonic frequencies. *Phys. Rev.* 75:936–946.

32. Thomas, V., A. J. Giacomin, and A. Wolfenden. 1994. A rheometer to measure the viscoelastic properties of polymer melts at ultrasonic frequencies. *Rev. Sci. Instrum.* 65:2395–2401.

33. Kanazawa, K. K., and J. G. Gordon 2nd. 1985. The oscillation frequency of a quartz resonator in contact with a liquid. *Anal. Chim. Acta.* 175:99–105.

34. Aklonis, J. J., and W. J. MacKnight. 1983. Introduction to Polymer Viscoelasticity. Wiley Interscience, New York.

35. Rouse, P. E., Jr. 1953. A theory of the linear viscoelastic properties of dilute solutions of coiling polymers. *J. Chem. Phys.* 21:1272–1280.

36. Ferry, J. D. 1980. Viscoelastic Properties of Polymers. John Wiley & Sons, New York.

37. George, A., Y. Chiang, B. Guo, A. Arabshahi, Z. Cai, and W. W. Wilson. 1997. Second virial coefficient as predictor in protein crystal growth. *Methods Enzymol.* 276:100–110.

38. Rosenbaum, D. F., and C. F. Zukoski. 1996. Protein interaction and crystallization. *J. Cryst. Growth.* 169:752–758.

39. Demoruelle, K., B. Guo, S. Kao, M. McDonald Heather, B. Nikic Dragan, C. Holman Steven, and W. W. Wilson. 2002. Correlation between the osmotic second virial coefficient and solubility for equine serum albumin and ovalbumin. *Acta Crystallogr. D Biol. Crystallogr.* 58:1544–1548.

40. Valente, J. J., R. W. Payne, M. C. Manning, W. W. Wilson, and C. S. Henry. 2005. Colloidal behavior of proteins: Effects of the second virial coefficient on solubility, crystallization and aggregation of proteins in aqueous solution. *Curr. Pharm. Biotechnol.* 6:427–436.

41. Neal, B. L., D. Asthagiri, O. D. Velev, A. M. Lenhoff, and E. W. Kaler. 1999. Why is the osmotic second virial coefficient related to protein crystallization? *J. Cryst. Growth.* 196:377–387.

42. Curtis, R. A., J. M. Prausnitz, and H. W. Blanch. 1998. Protein-protein and protein-salt interactions in aqueous protein solutions containing concentrated electrolytes. *Biotechnol. Bioeng.* 57:11–21.

43. Zimm, B. H. 1946. Applications of the methods of molecular distribution to solutions of large molecules. *J. Chem. Phys.* 14:164–179.

44. Neal, B. L., D. Asthagiri, and A. M. Lenhoff. 1998. Molecular origins of osmotic second virial coefficients of proteins. *Biophys. J.* 75:2469–2477.

45. Davis-Searles, P. R., A. J. Saunders, D. A. Erie, D. J. Winzor, and G. J. Pielak. 2001. Interpreting the effects of small uncharged solutes on protein-folding equilibria. *Annu. Rev. Biophys. Biomol. Struct.* 30:271–306.

46. Mandel, M. 1993. Applications of dynamic light scattering to polyelectrolytes in solution. *In* Dynamic Light Scattering: The Method and Some Applications. W. Brown, editor. Oxford University Press, New York. 319–371.

47. Eberstein, W., Y. Georgalis, and W. Saenger. 1994. Molecular interactions in crystallizing lysozyme solutions studied by photon correlation spectroscopy. *J. Cryst. Growth.* 143:71–78.

48. Veldkamp, W. B., and J. R. Votano. 1976. Effects of intermolecular interaction on protein diffusion in solution. *J. Phys. Chem.* 80:2794–2801.

49. Andries, C., W. Guedens, J. Clauwaert, and H. Geerts. 1983. Photon and fluorescence correlation spectroscopy and light scattering of eye-lens proteins at moderate concentrations. *Biophys. J.* 43:345–354.

50. Narayanan, J., and X. Y. Liu. 2003. Protein interactions in undersaturated and supersaturated solutions: a study using light and x-ray scattering. *Biophys. J.* 84:523–532.

51. Zhang, J., and X. Y. Liu. 2003. Effect of protein-protein interactions on protein aggregation kinetics. *J. Chem. Phys.* 119:10972–10976.

52. Harding, S. E., and P. Johnson. 1985. The concentration-dependence of macromolecular parameters. *Biochem. J.* 231:543–547.

53. Pusey, P. N., and R. J. A. Tough. 1985. Particle interactions. *In* Dynamic Light Scattering: Applications of Photon Correlation Spectroscopy. R. Pecora, editor. Plenum Press, New York. 85–180.

54. Bajaj, H., V. K. Sharma, and D. S. Kalonia. 2004. Determination of second virial coefficient of proteins using a dual-detector cell for simultaneous measurement of scattered light intensity and concentration in SEC-HPLC. *Biophys. J.* 87:4048–4055.

55. David, C., M. C. Millot, E. Renard, and B. Sebille. 2002. Coupling of antibodies to b-cyclodextrin-coated gold surfaces via an intermediate adamantyl-modified carboxymethylated dextran layer. *J. Inclusion Phenom. Macro. Chem.* 44:369–372.

56. Lutanie, E., J. C. Voegel, P. Schaff, M. Freund, J. P. Cazenave, and A. Schmitt. 1992. Competitive adsorption of human immunoglobulin G and albumin: consequences for structure and reactivity of the adsorbed layer. *Proc. Natl. Acad. Sci. USA.* 89:9890–9894.

57. Lide, D. R. 2006. CRC Handbook of Chemistry and Physics. CRC Press, Boca Raton, FL.

58. Elcock, A. H., and J. A. McCammon. 2001. Calculation of weak protein-protein interactions: the pH dependence of the second virial coefficient. *Biophys. J.* 80:613–625.

59. Bermudez, O., and D. Forciniti. 2004. Aggregation and denaturation of antibodies: a capillary electrophoresis, dynamic light scattering, and aqueous two-phase partitioning study. *J. Chromatogr. B Analyt. Technol. Biomed. Life Sci.* 807:17–24.

60. Song, D., and D. Forciniti. 2001. Monte Carlo simulations of peptide adsorption on solid surfaces (Monte Carlo simulations of peptide adsorption). *J. Chem. Phys.* 115:8089–8100.

61. Placidi, M., and S. Cannistraro. 1998. A dynamic light scattering study on mutual diffusion coefficient of BSA in concentrated aqueous solutions. *Europhys. Lett.* 43:476–481.

62. Jones, R. B., and P. N. Pusey. 1991. Dynamics of suspended colloidal spheres. *Annu. Rev. Phys. Chem.* 42:137–169.

63. Ackerson, B. J. 1976. Correlations for interacting Brownian particles. *J. Chem. Phys.* 64:242–246.

64. Ackerson, B. J. 1978. Correlations for interacting Brownian particles. II. *J. Chem. Phys.* 69:684–690.

65. Muschol, M., and F. Rosenberger. 1995. Interactions in undersaturated and supersaturated lysozyme solutions: static and dynamic light scattering results. *J. Chem. Phys.* 103:10424–10432.